Assessing doping strategies for monolayer MoS2 towards non-enzymatic detection of cortisol: a first-principles study

Gabriele Boschetto, Aida Todri-Sanial

Assessing doping strategies for monolayer MoS_2 towards non-enzymatic detection of cortisol: a first-principles study

Gabriele Boschetto, and Aida Todri-Sanial

Laboratory of Computer Science, Robotics, and Microelectronics, University of Montpellier, CNRS, 161 Rue Ada, 34095 Montpellier, France.

E-mail: aida.todri@lirmm.fr

Abstract

In this work, we investigate by means of atomistic density functional theory simulations the interaction between cortisol (the target molecule) and monolayer MoS_2 (the substrate). The aim is to assess viable strategies for the non-enzymatic chemical sensing of cortisol. Metal doping of the sensing material could offer a way to improve the device response upon analyte adsorption, and could also enable novel and alternative detection mechanisms. For such reasons, we explore metal doping of MoS_2 with Ni, Pd, and Pt, as these are metal elements commonly used in experiments. Then, we study the material response from the structural, electronic, and charge-transfer points of view. Based on our results, we propose two possible sensing mechanisms and device architectures: i) a field-effect transistor, and ii) an electrochemical sensor. In the former, Ni-doped MoS_2 would act as the FET channel, and the sensing mechanism involves the variation of the surface electrostatic charge upon the adsorption of cortisol. In the latter, MoS_2 decorated with Pt nanoparticles could act as the working electrode, and the sensing mechanism would involve the reduction of cortisol. In addition, our findings may suggest the suitability of both doped and metal-doped MoS_2 as sensing layers in an optical sensor.

1 Introduction

Cortisol, or hydrocortisone if supplied as a medication, is a steroid hormone which plays a fundamental role in many physiological processes in both humans and animals. It is part of the glucocorticoid class of hormones, which means it is directly involved in the metabolism of glucose.[1] In addition, prolonged high levels of such hormone in the body lead to its active role also in the protein and lipid metabolism. Notably, cortisol is also an important actor in the stress and immune response: a correlation has been observed between sustained stress and high levels of circulating cortisol,[2, 3] so that it is often regarded as "the stress hormone". Other aspects that have been observed to be affected by cortisol levels are, for instance, bone formation[4] and memory.[5]

Being able to detect and measure the change in cortisol levels in the human body can aid in the general monitoring of human health and well-being:[6, 7] for instance, this could be useful for the early detection of cardiovascular diseases,[8] for the monitoring of a possible compromised immune state, and also for keeping track of the health condition of athletes during intense physical activities.[9] Therefore, in the context of Internet of Medical Things (IoMT),[10] there is currently a great interest in the development of innovative point-of-care biosensing devices that are able to detect and quantify cortisol in human biological samples.

Recently, atomically thin two-dimensional (2D) materials have been extensively studied to be used as biosensors, due to their unique mechanical, electrical, and optical properties.[11, 12] Although graphene is perhaps the most notable example of a 2D material, research is also currently focusing on transition-metal dichalcogenides (TMDs) such as molybdenum disulphide (MoS_2). Within the chemical space of TMDs, single-layer MoS_2 is one of the most studied materials due to its stability, direct optical band gap of $\sim$1.8 eV, and good carrier mobility, making it suitable for many optoelectronic applications.[13, 14, 15, 16, 17] Moreover, its properties can be fine-tuned, for instance, by both strain[18] and surface engineering (e.g., with the inclusion of defects, vacancies, and/or with doping). In the context of wearable electronics, single-layer MoS_2 could also be used for fabricating flexible devices,[19] thus paving the way for novel wearable point-of-care biosensors.[20]

In order to improve the sensitivity of the biosensor, a common technique is to modify (i.e., functionalize) the surface of the sensing material: this can be done either by binding an analyte-specific antibody/enzyme (enzymatic sensing) or by doping and/or by decorating the sensor's surface, typically with metallic nanoparticles or metal oxides (non-enzymatic sensing). The former strategy has the great advantage of providing devices with generally high selectivity towards the chosen analyte, however enzyme-based sensors are known to be rather unstable and prone to degradation to temperature and pH. On the other hand, non-enzymatic sensors can provide a higher stability and a prompt response, at the expense of a generally lower chemical selectivity.

A very popular biomarker for which many examples of both enzymatic and (to some extent) non-enzymatic biosen-

sors exist in the literature is glucose, whereas less is available regarding cortisol; moreover, most of the studied devices are enzymatic sensors. For instance, Kinnamon et al.[21] developed a portable biosensing device able to detect cortisol in human sweat: the authors have used MoS_2 nanosheets functionalized with a specific antibody. The electrochemical response of the sensor is modulated by the interaction of cortisol with such antibody. Sekar et al.[22] developed an enzymatic flexible electrochemical sensor based on conductive carbon fiber for the detection of cortisol in sweat samples. Gold nanoparticles have also been functionalized with cortisol-selective aptamers by Dalirirad et al.,[23] once again for the detection of cortisol in human sweat. Another aptamer-based cortisol biosensor has been studied by Fernandez et al.:[24] the method of detection involved the reduction reaction of the analyte, catalyzed by a copper metalloporphyrin (Cu-PP) ink attached to multi-walled carbon nanotubes. Recently, a non-enzymatic cortisol sensor has been proposed by Mugo et al.:[25] in their work the authors have used a polymer, poly(GMA-co-EGDMA), deposited on carbon nanotube-cellulose nanocrystals. The authors observed good performance and rapid analyte response.

The relatively smaller number of scientific publications on the topic, if compared to enzymatic sensing, clearly shows that non-enzymatic biosensing is a rather challenging task, from the point of view of both the sensing mechanism and the sensor development. Given the complexity of the topic, theoretical models can undoubtedly prove extremely useful in designing such devices, as models allow to shed light into the analyte/sensing material interaction and into the physical and chemical sensing mechanisms. To this end, atomistic modelling with density functional theory (DFT) has been widely used not only to study the interaction of small molecules (mainly gases) with the sensing materials,[26, 27, 28] but to some extent also to explore the sensing mechanism of somewhat "larger" biomolecules, like glucose and dopamine.[29, 30] However, to the best of our knowledge, the physico-chemical interaction between cortisol, which is a bigger and more complex molecule, and MoS_2 is still largely unexplored.

Therefore, the aim of this paper is to explore the interaction of cortisol with both doped and undoped MoS_2, in order to elucidate possible non-enzymatic sensing mechanisms. To do so, we used atomistic modelling with DFT to thoroughly investigate the cortisol/MoS_2 interaction from the point of view of structural, electronic, and charge transfer properties. We computed different figures of merit, such as band gaps, net atomic charges, and adsorption energies, in order to understand and quantify the nature and the strength of the interaction. We then studied the effect on such quantitites of common metal dopants, such as Ni, Pd, Pt, that have already been used for sensding purposes, either as point defects or in the form of nanoparticles.[31, 32, 33]

This paper is organized as follows: in Methods, the simulation details of the DFT calculations are described; in Results and Discussion, results on cortisol, metal-doped MoS_2, and their interaction are shown, together with their implications for the biosensing of cortisol. The Conclusions are then presented in the final section.

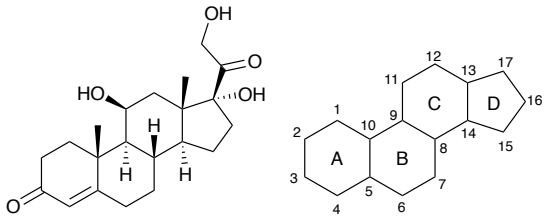

Figure 1: Chemical structure of cortisol (left), together with the carbon numbering and ring labels (right) that will be used throughout this work.

2 Methods

In this work, we explored the interaction of cortisol with both pristine and M-doped MoS_2. We chose three metal dopants commonly used for sensing applications: Ni, Pd, and Pt. To simulate metal-decorated MoS_2 sheets, we placed these metal atoms on top of the monolayer as adsorbed adatoms (non-substitutional doping). We placed cortisol on top of MoS_2 horizontally, in order to maximize the orbital overlap between the analyte and the sensing material.

Cortisol, being a steroid, is composed of four fused hydrocarbon rings, and possesses many possible binding and reactive sites, as can be observed from its chemical structure in Fig. 1. However, given previous reports[24, 34, 35] of the good reactivity of the carbonyl group directly attached to the ring A (carbon C-3), we decided to focus mainly on such moiety. Furthermore, our DFT simulations on isolated cortisol, presented in the following section, showed that the ring A of such molecule is particularly electron-rich, corroborating the data in the literature. Therefore, as the initial guess before performing the geometry optimization, we placed cortisol on top of doped MoS_2 so that the oxygen atom of the carbonyl group would sit above the metal dopant. When placing the analyte on top of the undoped monolayer, we ensured that the oxygen atom would sit above the Mo atom (top^{Mo}) in order for it to interact with the surrounding three S atoms, before carrying out a full geometry relaxation. To avoid the spurious interaction of cortisol with its periodic images, we considered a large orthorombic $8 \times 4 \times 1$ MoS_2 supercell with a total of 192 atoms, and with at least 15 Å of vacuum padding above and below the sheet. We also note that by choosing this large supercell we achieved a doping density of $\sim 1.8 \times 10^{13}$ cm^{-2}, within the range of typical doping values obtainable in experiments.[36]

Computer simulations were carried out at the DFT level by using QuantumATK R-2020.09[37, 38] atomic-scale modelling software. All simulations were performed in vacuum using the Perdew-Burke-Ernzerhof (PBE) exchange-correlation functional,[39] and to model core electrons we used norm-conserving pseudopotentials from the Pseu-

doDojo library.[40] We employed the LCAO approach with a density-mesh cut-off of 250 Ry, and we used the QuantumATK-optimized Medium basis set for geometry optimizations. The High basis set was used for single-point and properties calculations. We included dispersion effects by employing the D2 correction by Grimme.[41] Given the size of the simulation cell, we chose a **k**-point mesh defined by a $2\times2\times1$ Monkhorst-Pack (MP) grid,[42] whereas for computing the density of states (DOS) we employed a $4\times4\times1$ MP grid. All geometry optimizations were converged with residual atomic forces no larger than 0.03 eV/Å. We computed net atomic charges following the electron density partitioning scheme of the DDEC6 method, by using the CHARGEMOL program.[43] Differently from the widely used Mulliken population analysis, DDEC6 charges are independent of the basis set type and size, and have been shown to be chemically meaningful.[44, 45]

We defined the adsorption energy as:

$$E_{\text{ads}} = E_{\text{A+B}} - (E_{\text{A}} + E_{\text{B}}), \tag{1}$$

where $E_{\text{A+B}}$ is the total energy of the substrate and the adsorbate, whereas E_{A} and E_{B} are the total energies of the isolated fragments. For instance, when taking into consideration the adsorption of cortisol on (doped and undoped) MoS_2, $E_{\text{A+B}}$ would correspond to the total energy of the MoS_2/cortisol system, whereas E_{A} and E_{B} would be the total energies of MoS_2 and cortisol fragments, respectively. Finally, we took into account the basis set superposition error (BSSE) by including the counterpoise correction[46] in our total energy calculations.

3 Results and Discussion

3.1 Chemical Reactivity of Cortisol

We initially focused our efforts on the isolated cortisol molecule, in order to better understand its reactivity. The core structure of cortisol (see Fig. 1), common to the class of steroid hormones, consists of four fused carbon rings: rings A, B, and C are all 6-carbon rings, whereas ring D is composed of 5 carbon atoms. In addition, C-4 and C-5 in ring A are double-bonded. Attached to the core there are different functional groups, more specifically: two hydroxyl groups attached to C-11 and C-17, and one carbonyl group attached to C-3; attached to C-17 is also a small side chain which itself has both one hydroxyl and one carbonyl group. Intuitively, based on basic assumptions on its chemical structure, possible reactive centers of cortisol could be ring A and the side chain attached to ring D.

We first looked at the bond length of some of the potential reactive sites of the molecule: we first observed that the bond length of the carbonyl group at C-3 is slightly longer –and therefore the bond strength slightly weaker– than that at the side chain (1.24 Å and 1.22 Å, respectively). We also found that the C4=C5 double bond, whose length is 1.36 Å, is slighlty longer than the typical C=C double bond length

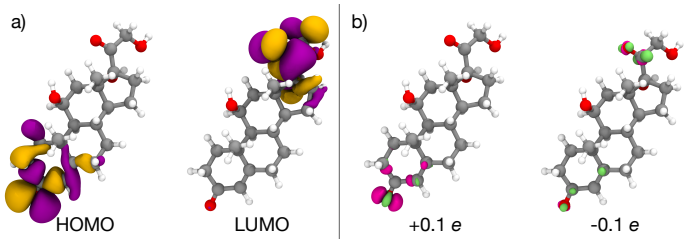

Figure 2: (a) Frontier orbitals of cortisol, isovalue 0.02 eV/Å^3. (b) EDD plots of cortisol, where magenta corresponds to electron depletion, whereas green to electron enrichment; isovalue 0.001 eV/Å^3. The numbers shown in the figure represent the total charge of the molecule: for instance, +0.1 e means that 0.1 electrons have been removed from the molecule.

of 1.34 Å. Further hints of the molecule's reactivity can be obtained by looking at its frontier orbitals, which are shown in Fig. 2. Interestingly, both HOMO and LUMO orbitals are strongly localized: the former mostly on the ring A, whereas the latter on the side chain and part of the ring D. This suggests that cortisol is characterized by an electron-rich donor part, the ring A, and an electron acceptor part, the side chain. To further confirm this finding, we artificially added and removed a small amount of charge (±0.1 e), and computed the electron density difference (EDD) for both positively- and negatively-charged cortisol; both plots are also shown in Fig. 2. Once again, it is possible to observe that the carbonyl group and the ring A overall act as an electron-donating group, whereas the carbonyl group attached on the side chain acts mainly as an electron-accepting group. However, for the negatively-charged molecule, we also note a slight increase of the electron density localized on the ring A. No variation of the electron density was observed on rings B and C.

Given these findings, together with the previously mentioned work from the literature, from this point onward we will focus our attention on the electron-rich ring A of cortisol, more specifically on the carbonyl group attached to it.

3.2 Electronic Properties of Metal-Decorated MoS_2

As one possible strategy to modulate the interaction between the analyte (cortisol) and the sensing material (MoS_2), we chose non-substitutional doping with three metal atoms, i.e., Ni, Pd, and Pt, adsorbed onto the MoS_2 surface. We chose these metal elements because of their increasing trend in the electronegativity (1.91, 2.20, 2.28 for Ni, Pd, and Pt, respectively), because they each belong to the $3d$ (Ni), $4d$ (Pd), and $5d$ (Pt) class of transition-metal compounds, and because such metallic species have already been used in experiments with MoS_2. We placed the adatoms at the top$^{\text{Mo}}$ adsorption site of MoS_2, i.e., above the Mo atom and at the center of three S atoms. From

Table 1: Summary of the structural, electronic, and charge-transfer properties of pristine and M-doped MoS_2. E_{ads} is the adsorption energy of the metal M on MoS_2, d_{M-Mo} and d_{M-S} are the bond lengths between the metal M and Mo or S atoms, respectively, ΔQ is the net charge transferred upon metal adsorption, Φ is the work function, and $E_{HOMO-LUMO}$ is the effective HOMO-LUMO gap; we point out that the latter is equal to the material's band gap only in the case of pristine MoS_2, whereas in the other three cases it simply represents the energy difference between the extra bands given by the metal dopants

Substrate	E_{ads} (eV)	d_{M-Mo} (Å)	d_{M-S} (Å)	ΔQ ($\|e\|$)	Φ (eV)	$E_{HOMO-LUMO}$ (eV)
MoS_2	-	-	-	-	5.16	1.77
Ni-MoS_2	-4.10	2.54	2.10	0.645	5.03	1.57
Pd-MoS_2	-2.66	2.83	2.34	0.367	5.09	1.65
Pt-MoS_2	-3.30	2.76	2.32	0.375	5.09	1.54

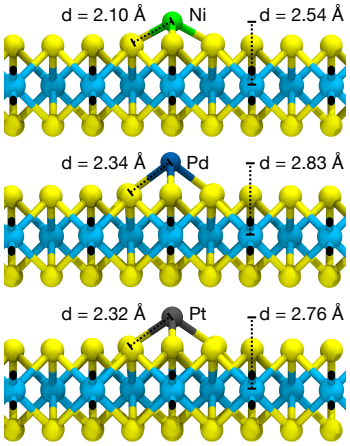

Figure 3: Chemical structures of metal-decorated MoS_2, zoomed in the proximity of the metal adsorption site. The figures represent, from top to bottom, Ni-MoS_2, Pd-MoS_2, and Pt-MoS_2. Relevant structural parameters, such as M-Mo and M-S distances, are shown.

this point onward, we will refer to the undoped material as pristine, whereas to the metal M-doped MoS_2 as Ni-MoS_2, Pd-MoS_2, and Pt-MoS_2, for each metal adatom respectively.

We investigated the effect of metal doping on the electronic properties of MoS_2, and we did so in terms of the structural, electronic, and charge-transfer properties. At first, we observed the interaction strength of Ni, Pd, and Pt with the surface of MoS_2 to be rather different. Ni is the element that chemically adsorbs on MoS_2 with the shortest bond lengths between Mo ($d_{Ni-Mo} = 2.54$ Å), and between the three surrounding S atoms ($d_{Ni-S} = 2.10$ Å). On the contrary, Pd is the element whose Pd-Mo ($d_{Pd-Mo} = 2.83$ Å) and Pd-S ($d_{Pd-S} = 2.34$ Å) bond lengths are the longest. Finally, we found that Pt leads to an intermediate behaviour ($d_{Pt-Mo} = 2.76$ Å, $d_{Pt-S} = 2.32$ Å). The chemical structures of doped-MoS_2, together with the bond length distances, are shown in Fig. 3. We expect such different bond lengths to correlate with the adsorption energy (E_{ads}) of the metal adatoms on the MoS_2 substrate: indeed, Ni leads to the strongest bonding with MoS_2, with a total adsorption energy of -4.10 eV, followed by Pt (-3.30 eV), and then Pd (-2.66 eV).

In terms of charge-transfer properties, we note that each metal adatom acts as an electron-donating compound to the MoS_2 substrate. The computed DDEC net atomic charges of these metal species were all found to be positive: we observed a value of $+0.645$ e, $+0.367$ e, and $+0.375$ e for Ni, Pd, and Pt, respectively. Once again, we note the significantly stronger interaction of Ni with respect to both Pd and Pt, and this correlates with the structural parameters discussed above. We expect this metal-to-substrate charge transfer to also impact the work function (Φ) of the material, that is, the minimum amount of energy to remove an electron from the substrate to the vacuum outside the material's surface. We computed this quantity for both the pristine and the doped materials by taking the chemical potential at a point in the vacuum, and we obtained a value of $\Phi_{MoS_2} = 5.16$ eV for MoS_2, in extremely good agreement with the experimental data of 5.15 eV.[47] All metal species were found to cause a slight decrease of this quantity, with $\Phi_{M-MoS_2} = 5.03$ eV, 5.09 eV, 5.09 eV for Ni, Pd, and Pt, respectively. This is consistent with the strenght of the metal-MoS_2 interaction and the amount of transferred charge. Moreover, we point out that such small decrease is most likely due to our relatively lower doping concentration with respect to other computational studies in the literature:[48] effectively, Ni causes a transfer of just 0.01 $|e|$ per MoS_2 formula, whereas for both Pd and Pt this value is only $\sim$0.006 $|e|$, thus confirming that the substrate is only weakly doped.

Finally, we also computed the projected density of states (PDOS) of each system, with projections onto the relevant atomic orbitals of S, Mo, and M (M = Ni, Pd, Pt), all shown in Fig. 4. As expected, in the PDOS of the pristine material the bands that give the largest contribution to the total DOS are those of the $2p$ orbitals of S atoms and of the $4d$ orbitals of Mo. We also note that our computed band gap of 1.77 eV matches well with the corresponding experimental value of $\sim$1.8 eV. Regarding the doped materials, results further confirm the weak doping effect, as the extra bands due to the metal adatoms are very close to the valence bands of MoS_2 (shallow-level doping). The difference in energy between the original valence band of MoS_2 and the extra highest occupied band of the dopant (the "new" material's HOMO) is rather small in each case, and is 0.21 eV, 0.15 eV, 0.15 eV for Ni-MoS_2, Pd-MoS_2, and Pt-MoS_2, respectively. Once again,

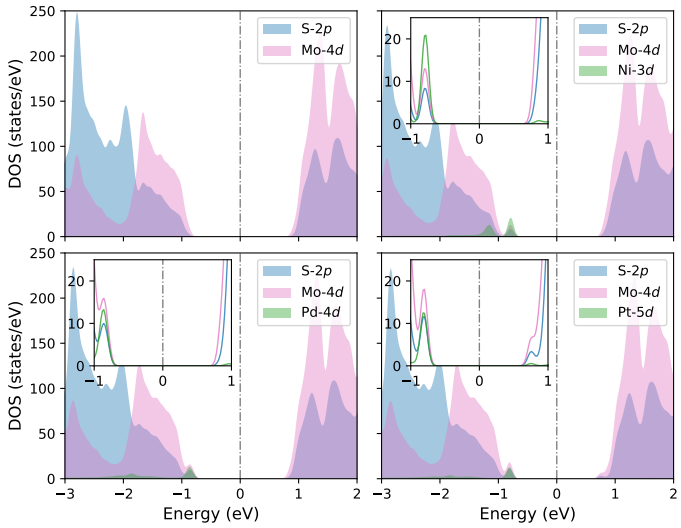

Figure 4: Projected density of states (PDOS) of pristine and M-doped MoS_2, centered around the Fermi level of each system. The projections are onto the relevant atomic orbitals of S, Mo, and M (M = Ni, Pd, Pt). Insets were added for clarity, and they show the zoomed area around the Fermi level, where the effect of metal doping becomes evident. The gaussian smearing is 0.05 eV.

this shows the stronger doping effect given by Ni. Interestingly, the effect of Pt also extends onto the conduction states of MoS_2, as can be seen from the (very low) extra shoulder which appears at the conduction band edge of Pt-MoS_2. For this band (the "new" material's LUMO), the energy difference with the original conduction band of the substrate is only 0.10 eV. However, as expected, doping does not cause any appreciable change in the band gap of the original material. From the PDOS, one can also observe that the 3*d*, 4*d*, and 5*d* orbitals of Ni, Pd, and Pt, respectively, overlap with both S-2*p* and Mo-4*d*, further indicating chemical bonding between the metal and the substrate. This is particularly evident for Ni, with clearly visible states further extending to lower energies.

To sum up, our simulation results on chemical bonds and charge transfer show that Ni has the strongest interaction with MoS_2, among the metal species considered in this study. A summary of all the computed structural, electronic, and charge-transfer properties discussed so far is shown in Table 1.

3.3 Cortisol Adsorption

3.3.1 Adsorption Mechanism.

We placed cortisol above the MoS_2 substrate (pristine and with metal doping) as described in the Methods section, and we fully relaxed the atomic coordinates of the systems taking into account dispersion forces at the PBE-D2 level.

We first looked at the analyte/substrate interaction from the structural point of view. We analyzed the formation/disruption of chemical bonds, and the variation of bond lengths and interatomic distances upon adsorption. The optimized geometries of each system are shown in Fig. 5. Results show the interaction between cortisol and pristine MoS_2 to be rather weak, as no significant atom displacement was observed neither in the substrate nor in the analyte. The average distance between the carbonyl O atom and the substrate was found to be ∼2.82 Å. In addition, we also notice that no bending and/or strain occur in MoS_2 upon the adsorption of cortisol. On the contrary, including metal adatoms as point defects led to stronger interactions with the analyte, as can be observed from the non-negligible atomic displacement mostly occurring in the ring A of cortisol and in the proximity of the metal species. The rather small interatomic distances between the metal M and the O atom of the carbonyl group (1.94 Å, 2.18 Å, 2.12 Å for Ni, Pd, and Pt, respectively) could hint to some type of chemical bonding. Interestingly, whereas Ni and Pd tend to bind mostly to the O atom, Pt shows a somewhat different reactivity, with a significant interaction also with the C-3 atom of the carbonyl group. From Fig. 5 one can observe that the Pt and O atoms are not positioned on the same vertical axis, as Pt moves closer to the C-3 atom (d_{Pt-C3} = 2.38 Å).

Further hints of chemical reactivity can be found by looking at the variation of the cortisol C=O bond length. This quantity increases from the initial 1.24 Å up to 1.28 Å, 1.27 Å, 1.31 Å with Ni, Pd, and Pt, respectively. We note that Pt-MoS_2 significantly weakens the C=O bond, which might suggest the partial activation of the carbonyl group, opening the path to its possible catalytic reduction. Finally, we also observed some variation in the metal M-Mo bond lengths of Ni-MoS_2 and Pt-MoS_2, which were both found to increase (Δd_{Ni-Mo} = 0.06 Å, Δd_{Pt-Mo} = 0.05 Å), whereas no change has been observed in Pd-MoS_2.

To further elucidate the adsorption mechanism, and to confirm the nature of the bonds, we also computed the electron localization function (ELF) for each system, shown in Fig. 6. From the image it is clear that the interaction between cortisol and pristine MoS_2 is purely given by dispersion forces, as the ELF ≈ 0 in between the two fragments. On the other hand, it is also clear that all metal adatoms M are chemically bound to the O atom of the carbonyl group, as ELF ≠ 0 in the M-O bond region. Moreover, the spatial localization of the ELF of Pt-MoS_2/cortisol confirms the strong interaction between Pt and C-3.

Finally, we quantified the interaction strength by computing the adsorption energy of each system. To gain the maximum amount of information, we decomposed the total adsorption energy (E_{ads}^{tot}) into its dispersion (E_{ads}^{disp}) and electrostatic (E_{ads}^{elec}) contributions. A summary of such quantities can be found in Table 3. As expected, when considering pristine MoS_2 we found E_{ads}^{tot} to be relatively low (-1.14 eV), and almost entirely depending on weak dispersion interactions (E_{ads}^{disp} = -1.27 eV). We also observed a repulsive electrostatic contribution (E_{ads}^{elec} = +0.13 eV) which weakens the overall adsorption energy. This confirms that, without any surface point defect, cortisol adsorbs on pristine MoS_2 via a

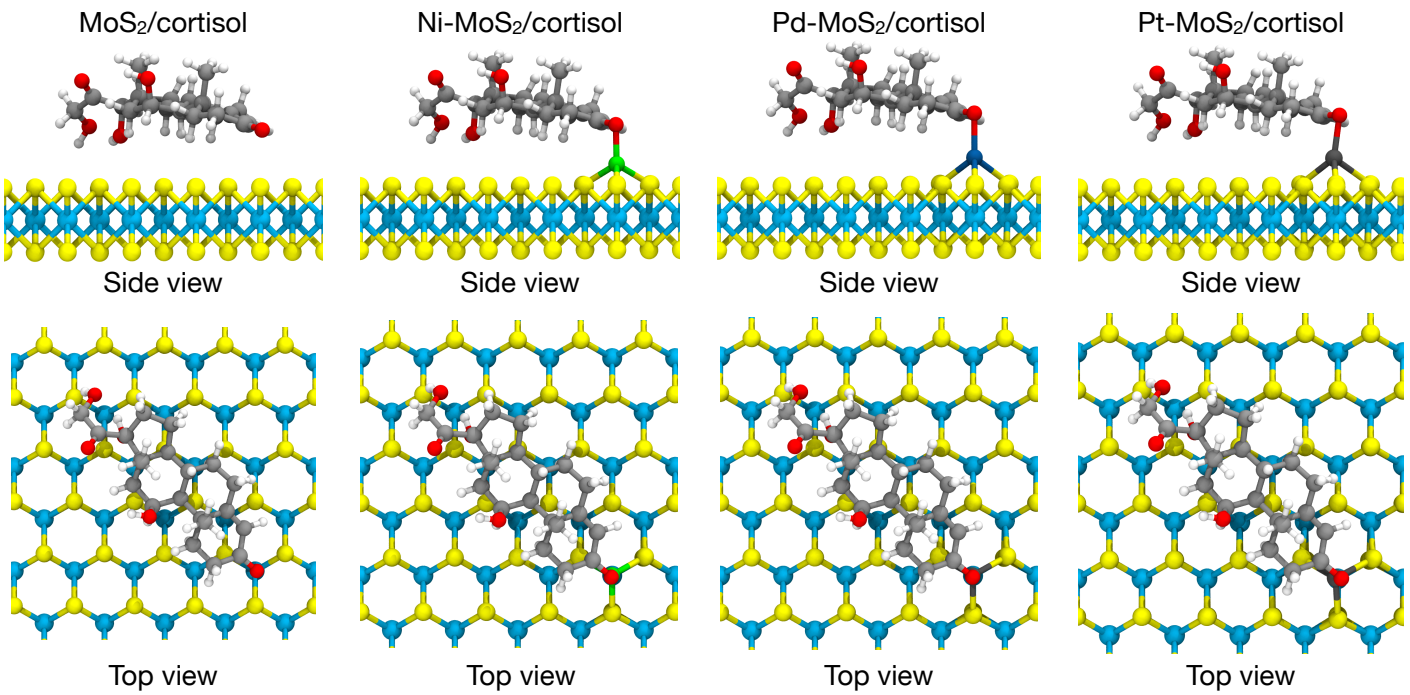

Figure 5: Optimized geometries (PBE-D2) of the MoS_2/cortisol systems considered in this paper, zoomed in the vicinity of the adsorption site (top and side views).

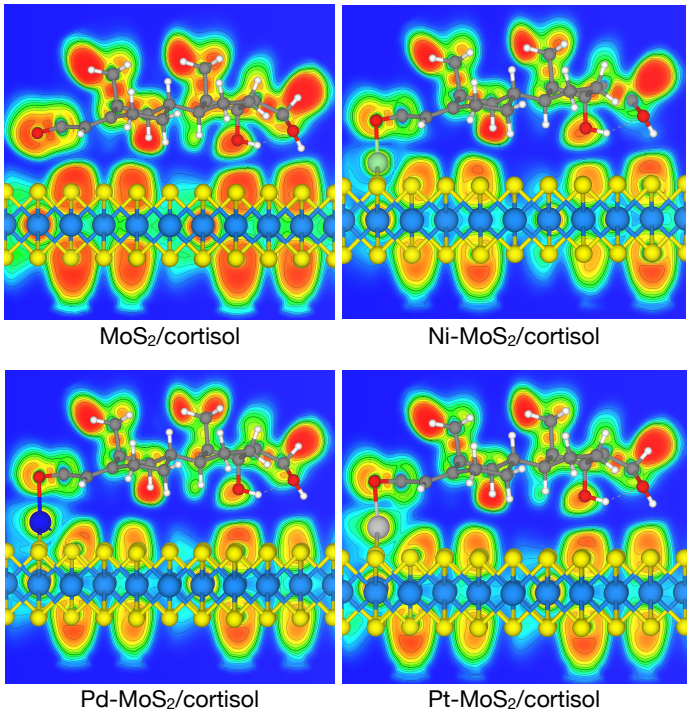

Figure 6: Electron localization function (ELF) of cortisol adsorbed on pristine and M-doped MoS_2, projected on a cut plane intersecting the carbonyl group of cortisol and the metal adatoms (Mo atom in the case of pristine MoS_2). Colour blue corresponds to ELF = 0, whereas colour red to ELF = 1.

physisorption mechanism. On the other hand, the inclusion of metal adatoms leads to significantly stronger adsorption energies: we found the highest value with Ni-MoS_2 (E_{ads}^{tot} = -2.21 eV), followed by Pt-MoS_2 (E_{ads}^{tot} = -2.15 eV), and then by Pd-MoS_2 (E_{ads}^{tot} = -1.72 eV). We also found that such stronger adsorption energies are due to both dispersion forces and attractive electrostatic interactions, confirming the occurring of chemical bonding. This is particularly evident for Pt-MoS_2, where E_{ads}^{elec} (-1.16 eV) accounts for more than half of the total adsorption energy. On the contrary, in the case of both Ni-MoS_2 and Pd-MoS_2, the electrostatic contribution is smaller than that of the dispersion forces, although still significant. We assume that such attractive electrostatic contribution in the case of Pt-MoS_2 is due to its tendency to react with both the O and the C-3 atoms of the carbonyl group, whereas Pd and Ni only bind to O, with a negligible interaction with C-3. Clearly, these results all point towards a chemisorption mechanism.

Overall, we can conclude that cortisol interacts with bare MoS_2 mainly via weak dispersion forces. When the substrate is doped, such interaction is dramatically improved by the chemical bonding of the analyte's ring A with the metal adatoms, locking the molecule onto the MoS_2 surface.

3.3.2 Charge Transfer and Charge Redistribution.

We investigated the electrostatic charge transfer occurring between the substrates and cortisol upon its adsorption, and we did so by computing the net atomic charges with the DDEC6 method. Also, to spatially visualize the charge redistribution, we computed the electron density difference

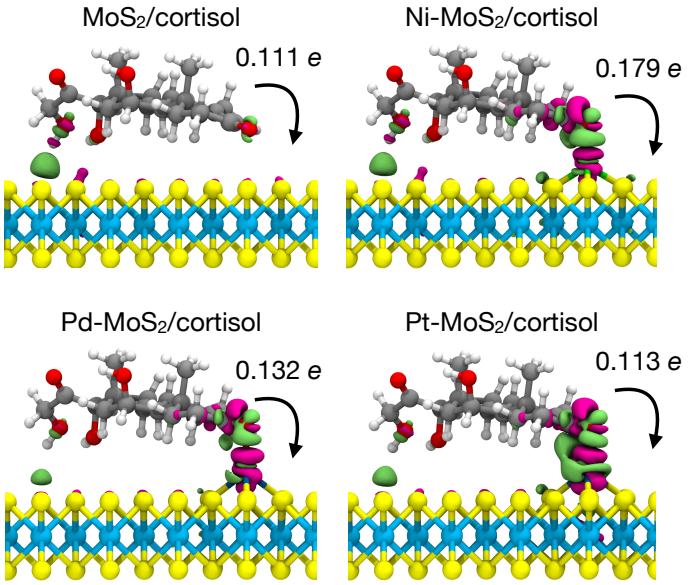

Figure 7: EDD maps of MoS_2 substrates upon adsorption of cortisol, zoomed in the proximity of the adsorption site. Magenta colour corresponds to electron depletion, whereas green colour to electron enrichment; isovalue 0.002 eV/Å^3. The amount of net charge transferred from cortisol to the substrate, computed with the DDEC6 method, is also shown.

Table 2: Net atomic charges of the relevant atoms of M-doped/cortisol systems, computed by means of the DDEC6 method. Q_i and Q_f are the atomic charges before and after the adsorption of cortisol, respectively. We note that to be consistent with the EDD maps, we performed the population analysis on single fragments in the geometry of the complex

Atom	Q_i (e)	Q_f (e)
	Ni-MoS_2/cortisol	
Mo	+0.437	+0.421
Ni	+0.644	+0.651
O	−0.485	−0.440
C-3	+0.439	+0.428
C-4	−0.307	−0.314
C-5	+0.136	+0.178
	Pd-MoS_2/cortisol	
Mo	+0.464	+0.454
Pd	+0.363	+0.415
O	−0.482	−0.439
C-3	+0.443	+0.423
C-4	−0.308	−0.318
C-5	+0.138	+0.172
	Pt-MoS_2/cortisol	
Mo	+0.456	+0.435
Pt	+0.353	+0.405
O	−0.487	−0.408
C-3	+0.433	+0.374
C-4	−0.304	−0.307
C-5	+0.134	+0.155

(EDD) map of each system. Our charge analysis showed that, overall, cortisol acts as a charge donating molecule, and we observed such behaviour with both undoped and doped MoS_2. From a quantitative point of view, we found a net non-negligible charge transferred (ΔQ) of 0.111 e with pristine MoS_2. Interestingly, we observed that not all metal dopants brought a significant increase of such quantity: overall, Ni-MoS_2 led to $\Delta Q = 0.179$ e, Pt-MoS_2 to $\Delta Q = 0.113$ e, and Pd-MoS_2 to $\Delta Q = 0.132$ e. These results show that Ni is the metal dopant which leads to a higher charge transferred from cortisol to the substrate, whereas with Pd the improvement is visible, although not significant. On the other hand, Pt does not seem to bring any improvement on ΔQ with respect to the pristine material.

EDD maps can also aid to better visualize the charge redistribution upon the adsorption of cortisol. From Fig. 7 it is possible to observe that the charge redistribution with pristine MoS_2 is rather limited, and spatially localized mainly in the area in the proximity of the side chain of cortisol. Here, the tail seems to act as a charge donating unit. On the contrary, we note very little charge redistribution on the other side of the molecule, that is, ring A. The situation is dramatically different with M-doped MoS_2: we observe a great charge redistribution in the region between the cortisol carbonyl group and the metal adatom, consistently with our previous results indicating the occurring of chemical bonding. EDD maps suggest that the metal adatoms generally act as charge donating units, whereas in the ring A of cortisol the charge appears to get mostly redistributed. Interestingly, we note that with Pt-MoS_2 the charge recombination is somewhat more spatially delocalized, with some significant electron enrichment in the area between Pt and the C-3 atom of cortisol. Once again, this points to the increased reactivity of the metal adatom towards the carbon atom of the carbonyl group. We point out that a greater charge recombination does not necessary lead to an increased charge transfer between the substrate and the adsorbate, as ultimately what matters is only the net transferred amount. In particular, with large molecules like cortisol, it is highly probable for different parts of the analyte to act non-trivially as both charge donating and charge accepting units.

To further elucidate the flow of charge in the systems consisting of M-doped MoS_2, we looked at the variation of the atomic charge in selected atoms upon cortisol adsorption; results are shown in Table 2. For instance, we observed that metal adatoms all lose some amount of charge: 0.007 e, 0.052 e, and 0.052 e for Ni, Pd, and Pt, respectively. Sulphur atoms bound to the metal adatoms also generally lose charge. On the other hand, the Mo atom to which the adatoms are bound show a gain in electrons: 0.016 e, 0.010 e, 0.021 e in Ni-MoS_2, Pd-MoS_2, and Pt-MoS_2, respectively. Regarding the ring A of cortisol, we observed the atoms with the most significant charge variation being O, C-3, C-4, and C-5 (the reader is referred to Fig. 1 for the numbering scheme of C atoms). O and C-5 both lose charge, whereas C-3 and C-4 gain charge. Consistently with

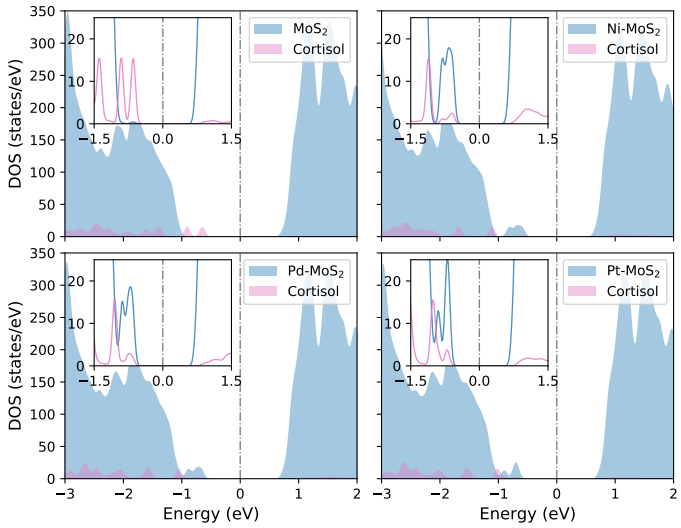

Figure 8: Projected density of states (PDOS) of cortisol adsorbed on pristine and M-doped MoS_2, centered around the Fermi level of each system. The projections are onto the MoS_2 and cortisol fragments. Insets were added for clarity, and they show the zoomed area around the Fermi level, where the effect of cortisol bound to the metal adatoms becomes evident. The gaussian smearing is 0.05 eV.

the increased reactivity of Pt towards the C-3 atom and the larger charge redistribution observed in the corresponding EDD map, we note a significant gain of charge in C-3 in the Pt-MoS_2/cortisol system.

Overall, results suggest that charge transfer and charge redistribution processes are non-trivial, given the complex interplay between charge donating and charge attracting units in the cortisol molecule. When cortisol is adsorbed on pristine MoS_2, the charge gets transferred mainly through the molecule's tail, whereas with M-doped MoS_2 the charge transfer occurs in the proximity of the M-O bond. Nevertheless, cortisol as a whole always acts as the charge donating fragment.

3.3.3 Electronic Structure Properties.

Finally, we looked at the change in the electronic structure of MoS_2 substrates upon cortisol adsorption. Fig. 8 shows the DOS of each system, projected onto both MoS_2 (doped and undoped) and cortisol fragments. DOS plots offer yet another mean to investigate the analyte/substrate interaction. The PDOS in Fig. 8 further confirm the different reactivity of cortisol with pristine and M-doped MoS_2: when the material is undoped no chemical interaction can be observed, as the DOS of MoS_2 does not change upon cortisol adsorption (the reader is referred to Fig. 4 for the DOS of the pristine materials without the adsorbed analyte). Moreover, the states found in the MoS_2 band gap region are due exclusively to the cortisol molecule, and therefore no variation in the band gap of MoS_2 occurs. This is corroborated by the bandstructure and the HOMO orbital plot of this system, which is localized exclusively on cortisol (see Fig. S1 in Supplementary Information).

On the other hand, from previous results showing chemical reactivity between cortisol and M-doped MoS_2, we expect to observe some changes in the DOS of the substrate: indeed, when comparing the DOS of metal-decorated MoS_2 before (Fig. 4) and after the adsorption of cortisol (Fig. 8), we note the appearance of extra bands in the band gap region of the substrate. These broaden the original bands due to the metal elements. As expected, in such extra bands hybridization between the states of cortisol and those of the M-doped materials can be observed. Once again, this is corroborated by the bandstructures and the HOMO orbital plots of the M-doped systems (see Figs. S2-S4 in Supplementary Information). Interestingly, when cortisol chemically adsorbs to Pt-MoS_2 we also observe the removal of the band near the conduction states of the substrate, which was due to Pt doping.

Although overall no appreciable change in the band gap of the MoS_2 substrates can be observed, we note that the extra bands due to the adsorption of cortisol lead to a smaller effective HOMO-LUMO gap ($E_{\mathrm{HOMO-LUMO}}$): we observe a variation of $E_{\mathrm{HOMO-LUMO}}$ of 0.40 eV, 0.33 eV, 0.26 eV, and 0.14 eV for pristine, Ni-decorated, Pd-decorated, and Pt-decorated MoS_2, respectively. Among the M-doped substrates, Ni-MoS_2 shows the largest change, whereas Pt-MoS_2 the smallest. This is due to a compensating effect between the removal of the near-conduction doping band and the broadening of the near-valence bands.

3.3.4 Sensing Mechanisms.

Here, we discuss the possible sensing mechanisms of cortisol, taking into account the results presented so far, summarized in Table 3. The design of the sensor would vary depending on the type of signal (see Fig. 9), which could be measured either by physical, chemical, or optical means.

One obvious sensing strategy would be the detection of the electrostatic charge transferred upon the adsorption of cortisol on the monolayer MoS_2 substrate. This can be achieved, for instance, with a field-effect transistor (FET):[49] the working mechanism first involves the adsorption of the analyte onto the sensing material (i.e., the channel in a FET); this causes the transfer of a certain amount of charge to the latter. In turn, this will lead to a variation of the surface electrostatic potential of MoS_2, and to a change in the measured device current. Essentially, cortisol would modulate the threshold gate voltage (V_{th}) of the device, thus enabling the detection of an electrical signal. For this type of device, results suggest Ni to be the best metal dopant (among those tested in the present work) as it significantly enhances the cortisol-to-MoS_2 charge transfer, and in turn the sensitivity of the device.

Another possible sensing mechanism which involves the transfer of charge could be enabled by the catalytic reduction of the carbonyl group of cortisol in C-3. In this situation, the redox reaction would cause a variation of the

Table 3: Summary of the electronic and charge transfer properties of cortisol adsorbed on pristine and M-doped MoS_2. E_{ads}^{tot} is the total adsorption energy, decomposed into its dispersion (E_{ads}^{disp}) and electrostatic (E_{ads}^{elec}) contributions. ΔQ is the net charge transferred upon cortisol adsorption, and $E_{HOMO-LUMO}$ is the effective HOMO-LUMO gap, which simply represents the energy difference of the extra bands given by doping and/or the adsorption of cortisol

Substrate/analyte	E_{ads}^{tot} (eV)	E_{ads}^{disp} (eV)	E_{ads}^{elec} (eV)	ΔQ ($\|e\|$)	$E_{HOMO-LUMO}$ (eV)
MoS_2/cortisol	-1.14	-1.27	+0.13	0.111	1.37
Ni-MoS_2/cortisol	-2.21	-1.33	-0.88	0.179	1.24
Pd-MoS_2/cortisol	-1.72	-0.99	-0.73	0.132	1.39
Pt-MoS_2/cortisol	-2.15	-0.99	-1.16	0.113	1.40

electric current passing through the device, which can be detected and measured. A similar sensing mechanism has been proposed for the non-enzymatic detection of glucose, achieved via its catalytic oxidation using NiO-decorated MoS_2.[50] In our study, for such purpose Pt might be a suitable doping material, given its strong reactivity towards the carbonyl group of cortisol: as previously discussed, we found this metal element to donate a significant amount of charge to C-3, which leads to the strongest weakening of the C=O double bond. In addition to single-atom doping, decorating MoS_2 surface with Pt nanoparticles may be a viable alternative that could be explored.

Finally, our results also suggest that optical methods could offer yet another alternative route for cortisol biosensing. Results showed that the adsorption of cortisol on MoS_2 substrate causes a number of near-valence extra states inside the MoS_2 band gap. These are purely due to cortisol for the pristine substrate, whereas for the M-doped substrates such states have hybrid character. The appearance of these states causes a decrease of the effective HOMO-LUMO gap of the MoS_2/cortisol systems, which could be detected via optical means. On the one hand, with pristine MoS_2 we expect to observe a series of charge-transfer excitations from cortisol to the substrate, as suggested by the PDOS plot in Fig. 8. Such excitations would lead to a small add-on shoulder to the MoS_2 optical spectrum, which can be detected, for instance, with photoluminescence. On the other hand, the optical spectra of M-doped MoS_2 would already present small extra shoulders due to doping, and therefore in this case the sensing can be achieved by measuring the shift of these shoulders upon the adsorption of the analyte. Ni, Pd, and Pt all causes a decrease in the effective HOMO-LUMO gap of the sytems, which would reflect in the red shift of the shoulders. Once again, Ni seems to perform better than the other metal dopants here considered, as it leads to the highest decrease of the effective gap, $\Delta E_{HOMO-LUMO} = 0.33$ eV, thus leading to the strongest red shift.

As a final note, we observed that all the metal dopants cause an increase in the adsorption energy of cortisol, which in principle would be detrimental for the reusability of the biosensor. Nevertheless, we point out that a stronger interaction would also probably correlate with a higher device sensitivity, and therefore this is a trade-off that has to be carefully taken into consideration. In order to restore the device, a possible strategy could be to remove the analyte, for instance, thermally.

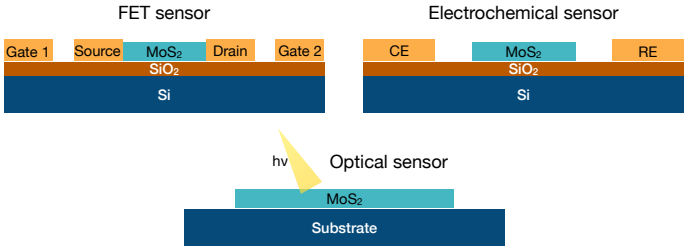

Figure 9: Schematics of FET, electrochemical, and optical sensors based on monolayer MoS_2. In the FET sensor, MoS_2 acts as the channel, whereas in the electrochemical sensor as the working electrode (WE). CE represents the counter electrode, and RE the reference electrode.

4 Conclusions

In summary, we used density functional theory simulations to explore the interaction between cortisol and MoS_2, both in its pristine state and metal-decorated with Ni, Pd, and Pt. Our aim was to assess the possibility of using commonly experimentally employed metal adatoms as a mean to modulate such interaction towards the non-enzymatic detection of cortisol.

4.1 Chemical Reactivity of Cortisol and Electronic Properties of MoS_2

We first focused on the substrate (MoS_2) and the analyte (cortisol) separately. Based on the electron density difference maps, we found that cortisol has two main reactive centers, its ring A and the tail attached to the ring D (see Figure 1). Moreover, we also found that the bond length of the carbonyl group in C-3 is slightly longer than that found in the side chain, suggesting that to be a possible reactive site. We note that also previous reports of cortisol sensing studies in the literature focused on the C=O group in C-3, and therefore, given our results and those found in the literature, we chose this carbonyl group as the reactive site of interest. We then explored the structural and electronic properties of M-doped MoS_2, and we found that all metal adatoms act as electron donating units to the substrate. Ni is the metal element with the strongest reactivity towards MoS_2, followed by Pt, and then Pd. This finding is based on the amount of charge transferred (+0.645 e of Ni with

respect to +0.367 e and +0.375 of Pd and Pt, respectively), and the adsorption energies (-4.10 eV with Ni against -2.66 eV and -3.30 eV with Pd and Pt, respectively). Moreover, from the structural point of view, Ni was found to have the shortest bond lengths with both S and Mo atoms. All the relevant structural, electronic, and charge transfer parameters of pristine and M-doped MoS_2 are summarized in Table 1.

4.2 Adsorption of Cortisol on MoS_2

We placed cortisol above both pristine and M-doped MoS_2 substrate, and we thoroughly studied the material response upon the analyte adsorption. Our results showed a weaker physisorption mechanism with pristine MoS_2, whereas a stronger chemisorption mechanism was found with the M-doped materials. We observed a significant increase of the adsorption energy with all metal adatoms, with non-negligible attractive electrostatic and dispersion forces. Furthermore, ELF, DOS, and EDD plots all suggested the formation of chemical bonds between the O atom of cortisol carbonyl group and the metal adatom. Interestingly, Pt showed enhanced reactivity also towards the C-3 atom of the carbonyl group, which led to a significant weakening of the C=O double bond, thus possibly activating such functional group for its catalytic reduction. In terms of charge transfer properties, we found that cortisol always acts as the electron donating unit towards the substrate, both pristine and M-doped, at least with the metal elements tested in this study. Ni-MoS_2 was the substrate which showed the largest amount of charge transferred, whereas with Pt-MoS_2 the charge transferred was comparable to that of undoped MoS_2, despite a large electron density redistribution in proximity of the Pt-O bond. These results suggest that the mechanism of charge transfer between cortisol and the substrate is not trivial, as the molecule is rather complex and relatively large, and therefore different parts of cortisol were found to react differently towards MoS_2. Furthermore, here we note that theoretical modelling is crucial, as it would be rather challenging to know a priori whether a metal element would enhance or not the cortisol-to-MoS_2 charge transfer, and if so, the magnitude of such quantity. Finally, we looked at the change in the electronic properties of MoS_2 by computing the DOS plots, and we observed the appearance of extra states within the band gap region of the substrates: these are due only to cortisol with the pristine substrate, whereas the extra states showed hybrid character with the M-doped materials.

4.3 Chemical Sensing of Cortisol

Overall, our results suggested two main possible sensing mechanisms and device architectures that could be used for the non-enzymatic detection of cortisol: i) a field-effect transistor (FET) and ii) an electrochemical sensor. In the first proposed device, the change in the electrostatic surface charge of the MoS_2 channel can be detected and correlated to the adsorption of cortisol. For such device we propose Ni as the doping material, as it significantly enhances the charge transfer with respect to pristine MoS_2. In the second proposed device, the signal would derive from the catalytic reduction of cortisol upon its adsorption. In this case, MoS_2 decorated with Pt nanoparticles could be used as the working electrode, as our results might suggest. In addition, we found evidence suggesting that an optical sensor might also work, and the optical spectra could be measured, for instance, with photoluminescence. The adsorption of cortisol would produce either an extra low-intensity peak or a red shift of the peaks, depending on theabsence or presence of dopants in MoS_2.

4.4 Outlook

Clearly, we point out that in real devices external effects may also play a role, thus further complicating the analyte/substrate interaction: few examples could be the increase/decrease of temperature, the variation of the pH, and the presence of other analytes in the sample. Nevertheless, this study provides important insights into the mechanism of cortisol adsorption on monolayer MoS_2, both pristine and metal-doped, together with possible design strategies of the sensing device. Future work could involve the investigation of more complex sensing platforms, such as functionalized MoS_2 and supported metal nanoparticles. Thus, we expect our results to be the starting point for further investigations on the non-enzymatic detection of cortisol with 2D nanomaterial-based devices.

Conflicts of interest

There are no conflicts to declare.

Acknowledgements

The authors would like to thank Stefania Carapezzi for providing feedback and for many helpful discussions. The authors ackowledge funding from the European Union's Horizon 2020 research and innovation programme, EU H2020 SmartVista project (www.smartvista.eu), grant agreement No. 825114. All the simulations were carried out on the Occigen Supercomputer hosted at C.I.N.E.S. (Centre Informatique National de l'Enseignement Supérieur), based in Montpellier (France).

References

[1] M. J. de Leon, T. McRae, H. Rusinek, A. Convit, S. De Santi, C. Tarshish, J. Golomb, N. Volkow, K. Daisley, N. Orentreich, and B. McEwen. Cortisol reduces hippocampal glucose metabolism in normal elderly, but not in alzheimer's disease. *J. Clin. Endocrinol. Metab*, 82:3251–3259, 1997.

[2] B. S. McEwen. Protective and damaging effects of stress mediators. *N. Engl. J. Med.*, 338:171–179, 1998.

[3] H. M. Burke, M. C. Davis, C. Otte, and D. C. Mohr. Depression and cortisol responses to psychological stress: A meta-analysis. *Psychoneuroendocrinology*, 30:846–856, 2005.

[4] Y. S. Chyun, B. E. Kream, and L. G. Raisz. Cortisol decreases bone formation by inhibiting periosteal cell proliferation. *Endocrinology*, 114:477–480, 1984.

[5] J. W. Newcomer, G. Selke, A. K. Melson, T. Hershey, S. Craft, K. Richards, and A. L. Alderson. Decreased memory performance in healthy humans induced by stress-level cortisol treatment. *JAMA Psychiatry*, 56:527–533, 1999.

[6] D. H. Hellhammer, S. Wüst, and B. M. Kudielka. Salivary cortisol as a biomarker in stress research. *Psychoneuroendocrinology*, 34:163–171, 2009.

[7] E. Russell, G. Koren, M. Rieder, and S. Van Uum. Hair cortisol as a biological marker of chronic stress: Current status, future directions and unanswered questions. *Psychoneuroendocrinology*, 37:589–601, 2012.

[8] E. Iob and A. Steptoe. Cardiovascular disease and hair cortisol: a novel biomarker of chronic stress. *Curr. Cardiol. Rep.*, 21:116, 2019.

[9] D. R. Seshadri, R. T. Li, J. E. Voos, J. R. Rowbottom, C. M. Alfes, C. A. Zorman, and C. K. Drummond. Wearable sensors for monitoring the physiological and biochemical profile of the athlete. *NPJ Digit. Med.*, 2:72, 2019.

[10] C. A. da Costa, C. F. Pasluosta, B. Eskofier, D. Bandeira da Silva, and C. da Rosa Righi. Internet of health things: Toward intelligent vital signs monitoring in hospital wards. *Artif. Intell. Med.*, 89:61–69, 2018.

[11] Deji Akinwande, Christopher J. Brennan, J. Scott Bunch, Philip Egberts, Jonathan R. Felts, Huajian Gao, Rui Huang, Joon-Seok Kim, Teng Li, Yao Li, Kenneth M. Liechti, Nanshu Lu, Harold S. Park, Evan J. Reed, Peng Wang, Boris I. Yakobson, Teng Zhang, Yong-Wei Zhang, Yao Zhou, and Yong Zhu. A review on mechanics and mechanical properties of 2d materials—graphene and beyond. *Extreme Mech. Lett.*, 13:42–77, 2017.

[12] R. Mas-Ballesté, C. Gómez-Navarro, J. Gómez-Herrero, and F. Zamora. 2d materials: to graphene and beyond. *Nanoscale*, 3:20–30, 2011.

[13] T. Li and G. Galli. Electronic properties of MoS_2 nanoparticles. *J. Phys. Chem. C*, 111:16192–16196, 2007.

[14] B. W. H. Baugher, H. O. H. Churchill, Y. Yang, and P. Jarillo-Herrero. Intrinsic electronic transport properties of high-quality monolayer and bilayer MoS_2. *Nano Lett.*, 13:4212–4216, 2013.

[15] H. Schmidt, S. Wang, L. Chu, M. Toh, R. Kumar, W. Zhao, A. H. Castro Neto, K. Martin, S. Adam, B. Özyilmaz, and G. Eda. Transport properties of monolayer MoS_2 grown by chemical vapor deposition. *Nano Lett.*, 14:1909–1913, 2014.

[16] C. Yim, M. O'Brien, N. McEvoy, S. Winters, I. Mirza, J. G. Lunney, and G. S. Duesberg. Investigation of the optical properties of MoS_2 thin films using spectroscopic ellipsometry. *Appl. Phys. Lett.*, 104:103114, 2014.

[17] Z. Yu, Z.-Y. Ong, Li S., J.-B. X, G. Zhang, Y.-W. Zhang, Y. Shi, and X. Wang. Analyzing the carrier mobility in transition-metal dichalcogenide MoS_2 field-effect transistors. *Adv. Funct. Mater.*, 17:1604093, 2017.

[18] H. J. Conley, B. Wang, J. I. Ziegler, R. F. Haglund, S. T. Pantelides, and K. I. Bolotin. Bandgap engineering of strained monolayer and bilayer MoS_2. *Nano Lett.*, 13:3626–3630, 2013.

[19] M. Zou, Y. Ma, X. Yuan, Y. Hu, J. Liu, and Z. Jin. Flexible devices: from materials, architectures to applications. *J. Semicond.*, 39:011010, 2018.

[20] S. Barua, H. S. Dutta, S. Gogoi, R. Devi, and R. Khan. Nanostructured MoS_2-based advanced biosensors: A review. *ACS Appl. Nano Mater.*, 1:2–25, 2018.

[21] D. Kinnamon, R. Ghanta, K.-C. Lin, S. Muthukumar, and S. Prasad. Portable biosensor for monitoring cortisol in low-volume perspired human sweat. *Sci. Rep.*, 7:13312, 2017.

[22] M. Sekar, M. Pandiaraj, S. Bhansali, N. Ponpandian, and C. Viswanathan. Carbon fiber based electrochemical sensor for sweat cortisol measurement. *Sci. Rep.*, 9:403, 2019.

[23] S. Dalirirad and A. J. Steckl. Aptamer-based lateral flow assay for point of care cortisol detection in sweat. *Sens. Actuators B Chem.*, 283:79–86, 2019.

[24] R. E. Fernandez, Y. Umasankar, P. Manickam, Nickel J. C., L. R. Iwasaki, B. K. Kawamoto, K. C. Todoki, J. M. Scott, and S. Bhansali. Disposable aptamer-sensor aided by magnetic nanoparticle enrichment for detection of salivary cortisol variations in obstructive sleep apnea patients. *Sci. Rep.*, 7:17992, 2017.

[25] S. M. Mugo and J. Alberkant. Flexible molecularly imprinted electrochemical sensor for cortisol monitoring in sweat. *Anal. Bioanal. Chem.*, 412:1825–1833, 2020.

[26] F. Mehmood and R. Patcher. Density functional theory study of chemical sensing on surfaces of single-layer MoS_2 and graphene. *J. Appl. Phys.*, 115:164302, 2014.

[27] Z. Zhang, K. Chen, Q. Zhao, M. Huang, and X. Ouyang. Effects of noble metal doping on hydrogen sensing performances of monolayer MoS_2. *Mater. Res. Express*, 7:015501, 2019.

[28] G. Cui, H. Zhang, X. Zhang, and J. Tang. Rh-doped $MoSe_2$ as a toxic gas scavenger: a first-principles study. *Nanoscale Adv.*, 1:772–780, 2019.

[29] J. Ortiz-Medina, F. López-Urías, H. Terrones, F. J. Rodríguez-Macías, M. Endo, and M. Terrones. Differential response of doped/defective graphene and dopamine to electric fields: A density functional theory study. *J. Phys. Chem. C*, 119:13972–13978, 2015.

[30] Y. Lei, D. Butler, M. C. Lucking, F. Zhang, T. Xia, K. Fujisawa, T. Granzier-Nakajima, R. Cruz-Silva, M. Endo, H. Terrones, M. Terrones, and A. Ebrahimi. Single-atom doping of MoS_2 with manganese enables ultrasensitive detection of dopamine: Experimental and computational approach. *Sci. Adv.*, 6:eabc4250, 2020.

[31] D. Sarkar, X. Xie, J. Kang, H. Zhang, W. Liu, J. Navarrete, M. Moskovits, and K. Banerjee. Functionalization of transition metal dichalcogenides with metallic nanoparticles: Implications for doping and gas-sensing. *Nano Lett.*, 15:2852–2862, 2015.

[32] D. Ma, W. Ju, T. Li, X. Zhang, C. He, B. Ma, Y. Tang, Z. Lu, and Z. Yang. Modulating electronic, magnetic and chemical properties of MoS_2 monolayer sheets by substitutional doping with transition metals. *Appl. Surf. Sci.*, 364:181–189, 2016.

[33] W. He, Y. Huang, and J. Wu. Enzyme-free glucose biosensors based on MoS_2 nanocomposites. *Nanoscale Res. Lett.*, 15:60, 2020.

[34] N. Suda, H. Sunayama, Y. Kitayama, Y. Kamon, and T. Takeuchi. Oriented, molecularly imprinted cavities with dual binding sites for highly sensitive and selective recognition of cortisol. *R. Soc. open sci.*, 4:170300, 2017.

[35] P. Manickam, R. E. Fernandez, Y. Umasankar, M. Gurusamy, F. Arizaleta, G. Urizar, and S. Bhansali. Salivary cortisol analysis using metalloporphyrins and multi-walled carbon nanotubes nanocomposite functionalized electrodes. *Sens. Actuators B Chem.*, 274:47–53, 2018.

[36] P. Luo, F. Zhuge, Q. Zhang, Y. Chen, L. Lv, Y. Huang, H. Li, and T. Zhai. Doping engineering and functionalization of two-dimensional metal chalcogenides. *Nanoscale Horiz.*, 4:26–51, 2019.

[37] S. Smidstrup, T. Markussen, P. Vancraeyveld, J. Wellendorff, J. Schneider, T. Gunst, B. Verstichel, D. Stradi, P. A. Khomyakov, U. G. Vej-Hansen, et al. Quantumatk: An integrated platform of electronic and atomic-scale modelling tools. *J. Phys: Condens. Matter*, 32:015901, 2020.

[38] QuantumATK version R-2020.09, Synopsys QuantumATK (www.synopsys.com/silicon/quantumatk.html).

[39] J. P. Perdew, K. Burke, and M. Ernzerhof. Generalized gradient approximation made simple. *Phys. Rev. Lett.*, 77:3865–3868, 1996.

[40] M. J. van Setten, M. Giantomassi, E. Bousquet, M. J. Verstraete, D. R. Hamann, X. Gonze, and G.-M. Rignanese. The pseudodojo: Training and grading a 85 element optimized norm-conserving pseudopotential table. *Comput. Phys. Commun.*, 226:39–54, 2018.

[41] Stefan Grimme. Semiempirical gga-type density functional constructed with a long-range dispersion correction. *J. Comput. Chem.*, 27(15):1787–1799, 2006.

[42] H. J. Monkhorst and J. D. Pack. Special points for brillouin-zone integrations. *Phys. Rev. B*, 13:5188–5192, 1976.

[43] T. A. Manz and N. Gabaldon Limas. Chargemol program for performing DDEC analysis, Version 3.5, 2017, (ddec.sourceforge.net).

[44] T. A. Manz and N. Gabaldon Limas. Introducing DDEC6 atomic population analysis: Part 1. charge partitioning theory and methodology. *RSC Adv.*, 6:47771–47801, 2016.

[45] T. A. Manz and N. Gabaldon Limas. Introducing [DDEC6 atomic population analysis: Part 2. computed results for a wide range of periodic and nonperiodic materials. *RSC Adv.*, 6:45727–45747, 2016.

[46] S. F. Boys and F. Bernardi. The calculation of small molecular interactions by the differences of separate total energies. some procedures with reduced errors. *Mol. Phys.*, 19:553–566, 1970.

[47] S. Choi, Z. Shaolin, and W. Yang. Layer-number-dependent work function of MoS_2 nanoflakes. *J. Korean Phys. Soc.*, 64:1550–1555, 2014.

[48] R. Costa-Amaral, A. Forhat, N. A. M. S. Caturello, and J. L. F. Da Silva. Unveiling the adsorption properties of 3d, 4d, and 5d metal adatoms on the MoS_2 monolayer: A dft-d3 investigation. *Surf. Sci.*, 701:121700, 2020.

[49] D. Sarkar, W. Liu, X. Xie, A. C. Anselmo, S. Mitragotri, and K. Banerjee. MoS_2 field-effect transistor for next-generation label-free biosensors. *ACS Nano*, 8:3992–4003, 2014.

[50] G. Jeevanandham, R. Jerome, N. Murugan, M. Preethika, K. Vediappan, and A. K. Sundramoorthy. Nickel oxide decorated MoS_2 nanosheet-based non-enzymatic sensor for the selective detection of glucose. *RSC Adv.*, 10:643–654, 2020.